Journal of MATERIALS RESEARCH

Article
DOI:10.1557/s43578-023-01225-0

Investigation of shape memory and mechanical properties of styrenic thermoplastic elastomer/PCL blends: Effect of blend composition

Emre Tekay[1,a)], Sinan Şen[1]

[1] Department of Polymer Materials Engineering, Yalova University, Yalova 77200, Turkey
[a)] Address all correspondence to this author. e-mail: emre.tekay@yalova.edu.tr

Received: 30 July 2023; accepted: 6 November 2023; published online: 15 November 2023

In this study, heat-responsive shape memory thermoplastic polymer blends were developed using a solution blending technique. The blends consisted of maleic anhydride grafted SEBS (SEBS-g-MA) as the elastomer phase and poly(caprolactone) (PCL) as the switch phase. The investigation focused on understanding the effects of blend composition on morphological and mechanical properties. Blends containing 40 and 50 wt % of PCL (SEBS60 and SEBS50, respectively) exhibited a co-continuous morphology. Increasing the PCL content led to higher Young's modulus and storage modulus at room temperature, while decreasing the creep strain. Shape-memory tests demonstrated promising results, with shape fixing ratios (R_f) reaching up to 98.54% and shape recovery ratios (R_r) up to 84.01%. Notably, the SEBS60 blend displayed the best shape-memory performance, achieving an R_f value of 97.15% and an R_r value of 76.29%. Cyclic shape-memory tests for the same blend maintained R_f values above 96% and R_r values above 82%.

Introduction

Smart materials form an important part of modern material research. Stimulant-sensitive polymers are materials that can significantly change their properties such as shape, mechanical properties, phase separation, optical properties, electrical properties, surface and permeability [1]. Among smart materials, shape memory polymers (SMPs), have a unique feature of changing their shape with help of a stimulus such as heat, chemicals, electricity, light and magnetic field [2]. The shape-memory effect relies on molecular movements at the micro scale. Heat-sensitive shape-memory polymers have stable molecules and restricted molecular movements when they are in their permanent shapes at low temperatures. The molecular motions increase at high temperatures, and in this case, when an external force is applied, the molecules are arranged to move to a lower entropy level by deformation. This entropic level is blocked and the temporal shape is fixed when the temperature is lowered. As the temperature is increased again, the molecular movements restart and the original shape is regained with the increase of entropy [3]. The temperature at which the temporary shape is retained is called the shape-fixing temperature (T_{fix}), and the temperature at which the permanent shape is recovered is referred to as the shape transition temperature (T_{trans}). These temperatures used in the shape memory effect are the melting temperature or the glass transition temperature, depending on the structure of the SMP [4]. The shape memory performance of a SMP is evaluated using shape fixing ratio (R_f) and shape recovery ratio (R_r) [5–7]. The R_f indicates the ability of the polymeric system to maintain its temporary shape during the shape fixation process, and R_r indicates the ability of the SMP to return to its permanent initial shape [8]. SMPs can be produced by two different methods as polymer synthesis and polymer blend preparation [9]. Multi-block copolymers, one of the basic classes of SMPs, consist of at least two different segments [10]. One of these segments is the elastomer segment with high T_g or T_m, and this component provides strength to the material above the transition temperature (T_{trans}). The other component is the switch segment, which has a lower thermal transition temperature and enables the temporary shape to be fixed. Synthesizing these multi-block copolymers is a difficult and complicated task, although it allows the development of novel SMPs. Compared to synthesizing block copolymers, the preparation of polymer blends containing an elastomer and a switch component is more feasible. The production of polymer

© The Author(s), under exclusive licence to The Materials Research Society 2023

blends is more diverse and the effect of environmental factors is lower during synthesis. On the other hand, shape memory performance can be easily determined by changing the blend composition [11]. Although covalently cross-linked rubbers can be used as the elastomer component responsible for shape recovery in the production of shape memory polymer blends, they are impossible to recycle and cause solid waste generation. As an alternative to these materials, thermoplastic elastomers (TPEs) offer advantages such as reprocessibility and recyclability [12]. Thermoplastic elastomers are copolymers composed of hard and soft blocks and exhibit phase-separated structures. The phases that make up TPEs are connected to each other by covalent bonds in the form of blocks or grafts. One of the phases has a high melting or glass transition temperature and is rigid at room temperature. The other phase consists of flexible chains with a low glass transition temperature and exhibits elastomeric properties at room temperature. Styrenic block copolymers (SBC), one of the most widely used TPEs, are triblock copolymers in A-B-A structure. Here, the block indicated by A is the hard phase polystyrene and B is the elastomeric block [13]. Poly (styrene-b-ethylene-butylene-b-styrene) (SEBS) block copolymer is a thermoplastic elastomer consisting of an elastomeric ethylene-butylene block in the middle and a rigid polystyrene block on both sides. The SEBS exhibits properties similar to conventional vulcanized rubbers at room temperature with this structure, but can be processed like thermoplastics at high temperatures because it does not have chemical crosslinks. Maleic anhydride grafted SEBS (SEBS-g-MA) is obtained by grafting polar maleic anhydride groups on nonpolar SEBS molecules. With this chemical structure, SEBS-g-MA can also interact with polar molecules compared to SEBS [14, 15]. PCL is a fully biocompatible and biodegradable semi-crystalline polymer and with these properties it is often used for biomedical purposes [16–18]. On the other hand, it is frequently used in the development of shape memory polymeric materials with its relatively low melting temperature and high toughness properties [19]. In the literature, shape memory polymer blends of PCL prepared with styrenic elastomers are quite limited. Abdallah et al. prepared a blend of PCL (40%) and styrene–butadiene–styrene (SBS) (60%) and investigated effect of enzymatic hydrolysis of the blend on mechanical and shape memory properties [3]. It is reported that the crystallinity degree, glass transition, and melting temperatures of PCL phase rise as M_w of PCL drops after the enzymatic hydrolysis of the blend. They also found that the R_r value of the PCL/SBS blend dropped as the Mw of PCL decreases. In another study of a PCL-based shape memory polymer blend using SBS elastomer [20], morphological and mechanical tests revealed a phase-separated morphology. The PCL started to develop a continuous phase after a 30% content level while its use in 70% caused "phase inversion". Based on the results of the shape memory tests, the optimal SMP blend was developed with an optimized morphological design that included SBS elastomer as the major continuous phase and PCL as a switch polymer as the minor continuous phase. Peng et al. produced 3D printable Recently, the only study using SEBS-g-MA and PCL together has been the production of carbon nanotube reinforced polymer nanocomposites with electro-active shape memory properties [21]. The thermo-responsive shape memory blends were also prepared with SEBS-g-MA elastomer and PCL switch component at different compositions via melt mixing method. The semicrystalline PCL as switch polymer was reported to keep the temporary shape of the blend below its T_m (60 °C) used as the T_{trans} of the SMP blend, and melt at 60 °C. The blend containing these components in equal amounts exhibiting co-continuous morphology resulted in maximum recovery and fixing ratios in shape memory performance test. In another study, Peng et al. compared the compression molding and 3D printing methods for shaping shape memory polymer blends of SEBS/PCL, which they prepared using the melt blending technique. They reported superior shape memory performance when using the 3D printing method and noted that the produced material exhibited self-healing properties at 80 °C [22].

In this project; the production of thermo-responsive shape memory SEBS-g-MA/PCL blends was carried out by solution mixing method unlike the abovementioned studies about thermo-responsive PCL/SBS or PCL/SEBS blends produced via melt mixing technique. In the production of shape memory polymer blends, PCL semi-crystalline polymer was used as switch polymer. It was thought that polar maleic anhydride functional groups on SEBS-g-MA polymer which is the elastomer component of the blend could interact with the PCL polymer having polar character. The blends were subjected to tensile tests and thermo-responsive shape memory test in tensile mode and the results were discussed in relation to the morphological properties of the blends and the blend composition. Dynamic mechanical analyses as well as creep performance tests of the blends were also done. Moreover, cyclic shape memory properties, temperature dependent shape recovery performances, shape memory of "U" shaped sample containing bending deformation as well as self-healing behavior of representative blend were also investigated.

Results and discussion

Morphological characterization of SEBS-g-MA/PCL blends

The distribution of polymer phases in the blend was determined by SEM analysis. The analyses were performed after etching the PCL phase from the cryo-fractured sample surfaces via dioxane. The SEM images of SEBS-g-MA/PCL blends are given in Fig. 1. The cavities in the images belong to etched PCL phase separated from the SEBS-g-MA elastomer phase. As it can be seen in the images, due to the incompatibility of the polymer components, all of the blends exhibited phase-separated

© The Author(s), under exclusive licence to The Materials Research Society 2023

morphology. However, it can be seen that the PCL phase shows a homogeneous distribution within the SEBS-g-MA phase in all of the blends. In Fig. 1(a)–(c) (SEBS90, SEBS80 and SEBS70, respectively), it is seen that the PCL phase was distributed discontinuously in the SEBS-g-MA phase and the size of the PCL domains increase with increase in the amount of PCL. In the SEBS60 blend [Fig. 1(d)], the PCL seemed to transform from discontinuous distribution morphology to a co-continuous morphology and similar morphology was observed for the SEBS50 polymer blend [Fig. 1(e)]. Obtaining co-continuous morphology in the blends is important for shape memory performance. Generally, the best shape performance effect in polymer blends is obtained in those with co-continuous morphology in which both phases can reflect their own properties.

DSC analyses of SEBS-g-MA/PCL blends

The DSC curves of the prepared SEBS-g-MA/PCL blends are presented in Fig. S1 (Supplementary Material File) and the results are tabulated in Table 1. DSC data for neat PCL were taken from a previous study [23]. In the blends, both the melting temperature and crystallization degree (X_c) of pure PCL showed a slight decrease in the presence of SEBS-g-MA (Table 1). This may be due to the inhibition of the crystallization process of PCL molecules by SEBS molecules as a result of the interaction

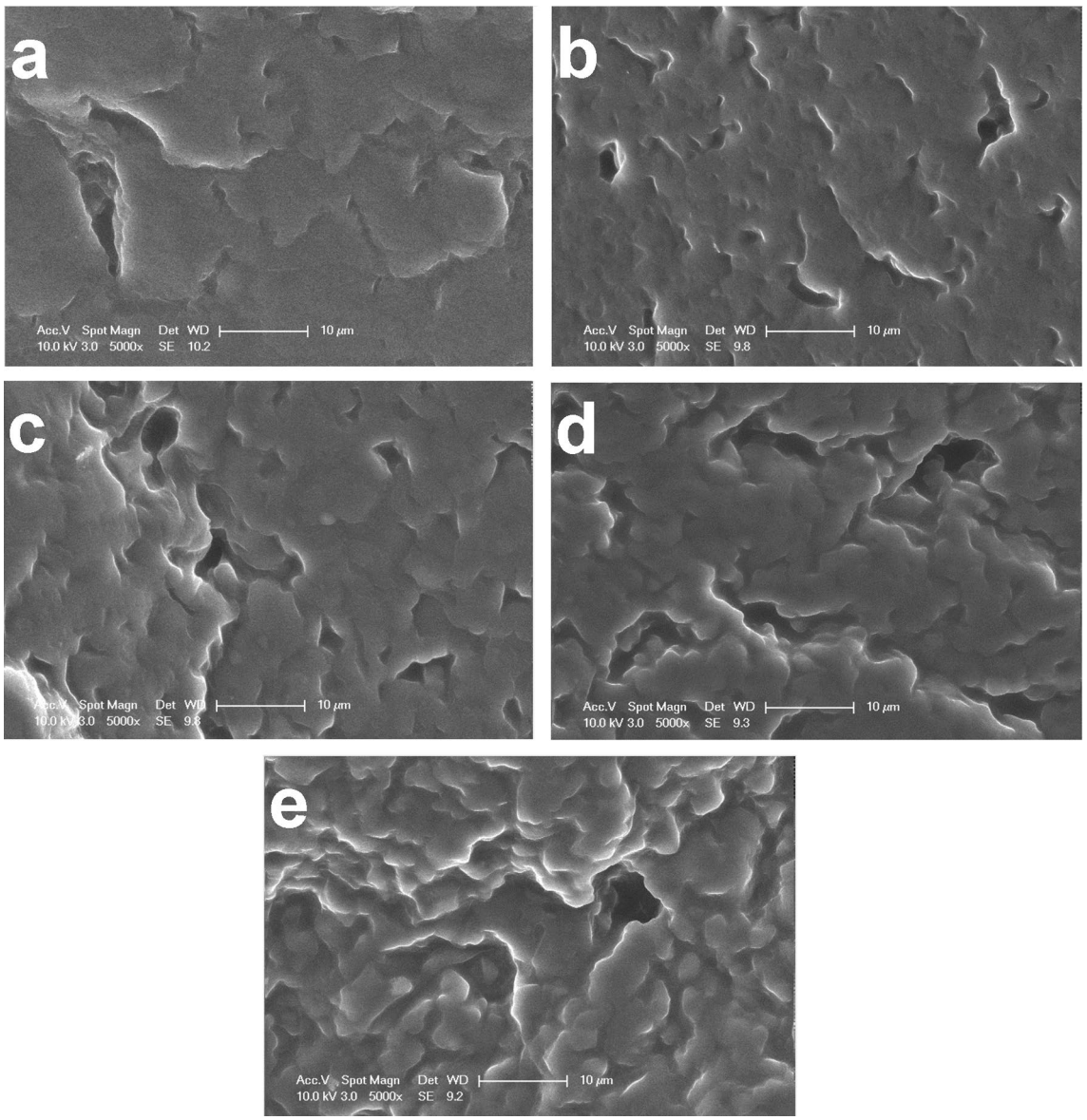

Figure 1: SEM images of SEBS-g-MA/PCL blends (a) SEBS90, (b) SEBS80, (c) SEBS70, (d) SEBS60 and (e) SEBS50.

© The Author(s), under exclusive licence to The Materials Research Society 2023

of PCL with polar maleic anhydride groups of SEBS-g-MA (Figs. S2 and S3, Supplementary Material File) [24–26]. The decrease in melting temperature and crystallinity can be attributed to the interactions between the polymers forming the polymer blends (Figs. S2 and S3, Supplementary Material File) [27]. In terms of thermal transitions of the SEBS-g-MA, it was found that PCL does not affect the Tg_{soft} and the Tc_{soft} of the ethylene-butylene block as well as the Tg_{hard} of the polystyrene block (Table 1). The melting temperature of the ethylene-butylene block (19.33 °C) increased slightly in the blends may have resulted from the restricted molecular movements of the ethylene-butylene chains as a result of the interactions of the polar groups of PCL with the MA groups of the SEBS-g-MA (Figs. S2 and S3, Supplementary Material File).

Since all of the SEBS-g-MA/PCL blends completed their melting processes before 60 °C (Fig. S1), this temperature value was chosen as the shape transition temperature (T_{trans}) to be used in the thermo-responsive shape memory behavior.

The crystallization temperature (T_c) of pure PCL (22.82 °C) shifted to higher temperature values as amount of SEBS-g-MA in the blends increases and reached 28.34 °C in the SEBS50 blend [Fig. S1(b) and Table 1]. The increases in the crystallization temperature of PCL in the blends may be ascribed to the polystyrene phase of the SEBS-g-MA, which is in solid form at crystallization temperature of the PCL, acting as a nucleating agent for the molten PCL molecules.

Another parameter important for the heat-triggered shape memory property is the shape-fixing temperature (T_{fix}), at which the transition of the switch component from the molten state to the solid state is completed and fixes the temporary shape of the material. Since all the SEBS-g-MA/PCL blends completed their crystallization above 10 °C, the T_{fix} at which temporary shape was fixed in the heat-triggered shape memory tests, was selected to be 10 °C.

Tensile properties of SEBS-g-MA/PCL blends

The stress–strain curves of the SEBS-g-MA/PCL blends are presented in Fig. S4 (Supplementary Material File), and the corresponding test results are shown in Table 2. Tensile data for neat PCL were taken from a previous study [23]. These polymer blends demonstrated high elongation at break values, elongating well beyond their original dimensions even at high drawing rates. They exhibited lower elongation than neat PCL but higher elongation than neat SEBS-g-MA elastomer, indicating that the phases are homogeneously dispersed in the blends. The SEBS90 blend exhibited a lower modulus (12.9 MPa) compared to that of SEBS-g-MA (18.5 MPa). This can be attributed to the interactions between the MA groups of SEBS-g-MA and PCL (Figs. S2 and S3, Supplementary Material File) in this particular composition, which may prevent clustering of the polystyrene blocks acting as physical crosslinking regions for the ethylene-butylene phases, thus reducing the stiffness of the matrix. In other compositions, as the amount of PCL (the rigid component in the blend) increased, the modulus value also increased. The highest modulus value was obtained in the SEBS50 blend, reaching 58.5 MPa.

All of the tensile strength values of the polymer blends took place within the range of those of the neat polymers, indicating the existence of interactions between polymer components

TABLE 1: The results of DSC analyses.

Materials	T_g (EB) (°C)	T_m (EB) (°C)	T_c (EB) (°C)	T_g (PS) (°C)	T_m (PCL) (°C)	T_c (PCL) (°C)	X_c (PCL) (%)
SEBS-g-MA	−55.32	19.33	0.30	89.55	–	–	–
SEBS90	−55.01	21.41	0.35	89.60	54.62	24.68	36.96
SEBS80	−54.32	22.15	0.31	89.22	56.48	25.41	36.09
SEBS70	−54.79	22.25	0.97	89.20	56.06	25.99	35.55
SEBS60	−55.46	22.41	0.77	89.55	56.77	27.94	35.30
SEBS50	−55.33	22.65	0.94	89.77	57.49	28.34	35.05
PCL	−64.89	–	–	–	57.22	22.82	40.19

TABLE 2: Tensile test data of SEBS-g-MA/PCL blends.

Materials	Elastic modulus (MPa)	Tensile strength (MPa)	Elongation at break (%)	Toughness (Nmm)
SEBS-g-MA	18.5 ± 3.0	6.72 ± 0.18	774 ± 13	12,796 ± 100
SEBS90	12.9 ± 2.1	9.49 ± 0.04	1129 ± 18	23,127 ± 674
SEBS80	20.2 ± 0.9	9.16 ± 0.25	1058 ± 37	23,266 ± 905
SEBS70	32.9 ± 2.9	10.02 ± 0.61	938 ± 57	22,468 ± 3029
SEBS60	41.4 ± 3.9	11.31 ± 0.27	1020 ± 21	31,174 ± 3610
SEBS50	58.5 ± 0.7	12.35 ± 0.21	1035 ± 19	35,274 ± 1446
PCL	156.0 ± 3.7	30.16 ± 0.64	1379 ± 16	85,908 ± 2380

© The Author(s), under exclusive licence to The Materials Research Society 2023

(Figs. S2 and S3, Supplementary Material File) and preventing early breakage. Likewise, all of the toughness values were found to be between the values of the pure polymer components. The toughness value of neat SEBS-g-MA (12,795.90 Nmm) increased with the increase in PCL amount and reached 35,274.49 Nmm in the SEBS50 polymer blend.

Creep properties of SEBS-g-MA/PCL blends

Creep tests of SEBS-g-MA/PCL materials were performed under 1 MPa stress and at 25 °C. The creep deformation vs. time curves are presented in Fig. 2(a) and the test results are tabulated in Table S1 (Supplementary Material File). Creep data for neat PCL were taken from a previous study [23]. It was found that neat PCL exhibits the lowest creep strain and the highest strain recovery [Fig. 2(a), Table S1] which can be ascribed to more elastic character of the PCL at 25 °C, as compared to SEBS-g-MA found at rubbery phase due to its EB phase with much lower T_g. The creep strain for the blends reduced as the amount of PCL, which is the hard component in the blend, increased except SEBS90 blend. This can be ascribed to restricted molecular movements of the SEBS elastomer by rigid PCL regions, slowing down the deformation of the SEBS molecules. Accordingly, the lowest creep strain was obtained in the SEBS50 blend. On the other hand, the higher creep strain of the SEBS90 blend compared to the neat SEBS-g-MA polymer can be explained by the lower elastic modulus of this polymer blend than SEBS-g-MA elastomer (Table 2). All the blends exhibited permanent deformations that increased in direct proportion to the creep strains they performed. Strain recovery percentages did not tend to change depending on the compositions, and all polymer blends showed greater than 80% recovery to their initial dimensions.

The creep analysis was repeated for the representative SEBS60 blend at temperatures of 35 and 45 °C. The related creep curves are given in Fig. 2(b) and the results of the analyses are presented in Table S2 (Supplementary Material File). As can be seen from the curves, the creep deformation increased with increase in the test temperature. As a result of the increase in the mobility of polymer molecules with the increase in the temperature, the softening of the material caused higher creep strain and permanent deformations accordingly. At 45 °C, a temperature close to the melting temperature of PCL, higher strain may occur due to the gradual increase in the energy of the PCL molecules and even some small crystals might have melted.

Dynamic mechanical properties of SEBS-g-MA/PCL blends

Figure S5 (Supplementary Material File) shows Tan δ vs. temperature and E' vs. temperature curves of SEBS-g-MA and PCL polymers. The DMA data for neat PCL were taken from a previous study [23]. The storage modulus-temperature and damping parameter-temperature graphs of SEBS-g-MA/PCL polymer blends are given in Fig. 3(a) and (b), respectively, and the results of the analyses are given in Table S3. The SEBS-g-MA is a triblock copolymer and therefore has two different glass transition temperatures (Fig. S5).

The glass transition temperature of the elastomeric ethylene-butylene block and that of the hard block polystyrene block was found to be − 49.3 and 90.61 °C, respectively. The T_g of PCL was determined as − 50.21 °C (Table S3). The decrease in E' of the PCL above 50 °C (Fig. S5, Supplementary Material File) is due to its melting transition at 57 °C (Table 1). All the polymer blends exhibited a single-step modulus drop and one tanδ peak (Fig. 3) since the glass transition temperatures of the ethylene-butylene block of SEBS and of PCL are very close to each other. In the polymer blends, the soft phase (EB) showed very few changes for its glass transition temperature (Table S3). The SEBS90 blend exhibited the lowest storage modulus and the highest damping at room temperature (25 °C) (Table S3), which

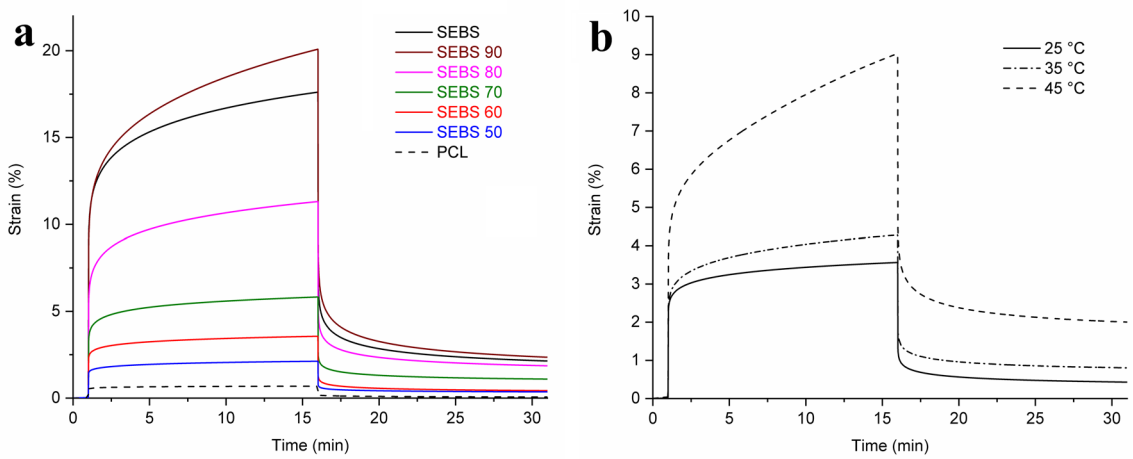

Figure 2: Creep test curves: (a) Creep curves of SEBS-g-MA/PCL blends and (b) Creep curves of SEBS 60 blend obtained at different temperatures.

© The Author(s), under exclusive licence to The Materials Research Society 2023

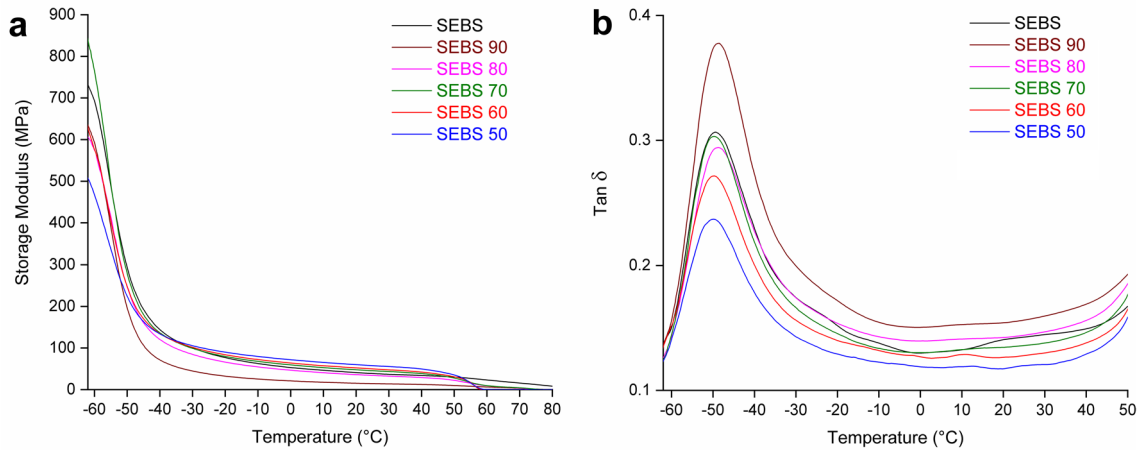

Figure 3: (a) Storage modulus vs. temperature and (b) Tanδ vs. temperature curves of SEBS-g-MA/PCL blends.

is in agreement with its lowest Young's modulus (Table 2) and the highest creep strain (Table S1) results. The lowest damping values in the glass transition region were obtained in the blends of SEBS60 and SEBS50 with the higher amounts of PCL and co-continuous morphologies. This may be ascribed to the rigid PCL phase restricting the movements of the ethylene-butylene elastomer segments of SEBS which limits their damping abilities. The storage moduli of the blends at 25 °C tended to increase directly with the amount of PCL while their damping values changed inversely with the amount of PCL (Table S3). This can be explained by the increased amounts of the crystalline structure at 25 °C with increase in PCL phase in the blends resulting in enhanced hardness and so restricted molecular movements reducing the damping performance. At 60 °C, which is above the melting temperature of PCL, sudden decreases were observed in the storage modulus values of the polymer blends compared to neat SEBS-g-MA as a result of melting of the crystal blocks of the PCL in the blends [Fig. 3(a)].

Thermo-responsive shape memory analyses of SEBS-g-MA/PCL blends

The thermo-responsive shape memory properties of the blends were investigated with the TMA instrument. First, the blends were heated to 60 °C as the shape transition temperature (T_{trans}), then they were subjected to 40–50% deformation at a constant force. After they were cooled to 10 °C (T_{fix}), the temporary shape was allowed to stabilize and then the applied force was removed to determine the material's temporary shape fixing ratio (R_f). The samples in their temporary shapes were again heated up to 60 °C and the shape recovery was monitored and at the end of the analyses, the shape recovery ratios (R_r) were calculated using the permanent deformation values on the materials.

The thermomechanical graphs from which the thermo-responsive shape memory performances of SEBS-g-MA/PCL polymer blends are determined, are given in Fig. 4 and the R_f and R_r values obtained from the graphs are presented in Table 3. In two-phase polymer blend systems consisting of elastomer and switch components, in general, shape recovery capability improves as the amount of elastomer phase increases and shape fixing performance improves as the amount of switch polymer phase increases [9]. It was found that the R_f ratios of SEBS-g-MA/PCL blends increased in direct proportion to the amount of PCL (Table 3). The lowest R_f was achieved for SEBS90 with 63.44% and the highest R_f was obtained in SEBS50 blend with 98.59% (Table 3). As the PCL content in the blend increased, the ability of the switch polymer phase to resist the entropic retraction force of the SEBS-g-MA elastomer improved and the polymer blends were able to maintain their temporary shapes to higher extents. On the other hand, as the amount of SEBS-g-MA in the blend increased, the shape recovery ratio (R_r) values improved except for SEBS90 blend. The lowest R_r was obtained in SEBS50 blend with 74.85% and the highest one was achieved in SEBS80 blend with 84.01%. The lower R_r ratio of the SEBS90 blend may be due to the fact that the initial deformation of this polymer blend is carried out by applying a higher force compared to other blends. The majority of the deformation applied to the SEBS 90 blend, which contains a small amount of molten PCL, may have occurred on the SEBS molecules. During the deformation, the PS blocks in the SEBS elastomer, which form a physical cross-link for the EB blocks, may have lost their positions by separating from each other and as a result of the relaxation of the molecules, the elastomer phase may have lost its properties and therefore a lower R_r ratio may have been obtained due to the decrease in the retraction force it will use for shape recovery [28]. It is known that apart from the effect of the composition of the components, the morphology of the components in the

© The Author(s), under exclusive licence to The Materials Research Society 2023

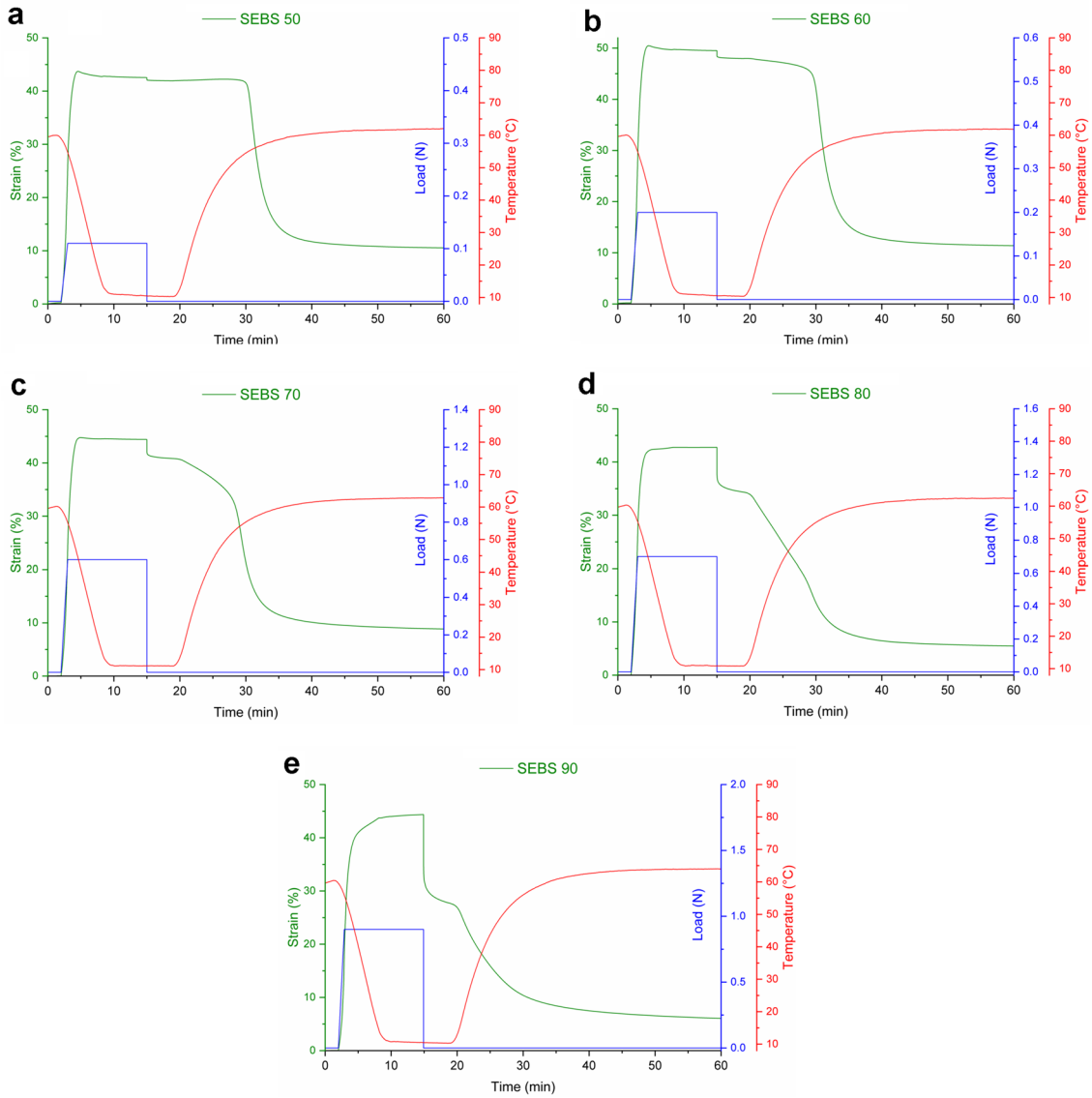

Figure 4: Thermomechanical shape memory curves of SEBS-g-MA/PCL blends: (a) SEBS 50, (b) SEBS 60, (c) SEBS 70, (d) SEBS 80 and (e) SEBS 90.

blend is also of great importance on the shape memory performances of SHP blends. Polymer blends with co-continuous morphologies allow both the elastomer component and switch component to retain their unique properties within the blend, so optimum shape memory performances are often achieved in compositions with this morphology. The co-continuous morphology is divided into (1) matrix elastomer phase and continuous switch phase and (2) matrix switch phase and continuous elastomer phase. It was reported that the systems in which the elastomer phase is the matrix and the continuous switch phase is distributed within this matrix exhibit better shape memory performances [20]. Among the blends, the SEBS60 has the same type co-continuous morphology with continuous PCL phase dispersed in the SEBS-g-MA elastomer phase. The optimum R_f and R_r values were obtained in this blend as compared to those of other SEBS-g-MA/PCL blends produced.

TABLE 3: Shape-memory properties of SEBS-g-MA/PCL polymer blends.

Materials	R_f (%)	R_r (%)
SEBS 50	98.59	74.85
SEBS 60	97.15	76.29
SEBS 70	92.34	78.31
SEBS 80	80.87	84.01
SEBS 90	63.44	78.17

Finally, the SEBS60 blend, which exhibits optimum shape memory with 97.15% shape fixing and 76.29% shape recovery

© The Author(s), under exclusive licence to The Materials Research Society 2023

ratios, was selected as the best performing blend and this composition was used for the further performance tests given in the following parts.

Shape memory properties of SEBS-g-MA/PCL polymer blends.

The potential of the SEBS60 as the representative blend to reproduce the shape memory properties was determined by thermomechanical analysis repeated cyclically three times. The analysis curve is presented in Fig. 5(a) and the R_f and R_r ratios obtained for each cycle are given in Table S4 (Supplementary Material File). In the analysis performed, although the same force was applied for each cycle, the deformation on the sample gradually increased. This increase in deformations is due to stress softening in cyclic deformations in elastomers or relaxation known as the Mullins effect. The Mullins effect is a phenomenon observed in elastomers (rubber-like materials) that exhibit a reduction in mechanical properties after being subjected to cyclic loading or deformation. This effect is characterized by the occurrence of various molecular-level changes, such as disentanglement, bond breakage, and molecular shifts within the elastomer molecules [29, 30]. The shape fixing and shape recovery performances of the blend in each cycle were compared and it was seen that as the number of cycles increases the R_f value increases while the R_r value decreases (Table S4). This change in the ratios also proves that SEBS-g-MA molecules relax as the number of cycle increases. It can be stated that stress softening occurs during deformation, leading to a reduction in the retraction force applied by the SEBS phase on the PCL phase during shape fixing, and resulting in a higher ratio of temporary shape fixing. On the other hand, due to the decrease in the retraction force provided by the elastomer phase, the ability to return to the permanent shape decreased and R_r values decreased during the shape recovery process. The reason for the higher R_r values obtained for cycle test (Table S4) in comparison with the R_r value given in the Table 3 for the same blend can be due to the fact that lower permanent deformations occur as a result of the application of lower strains on the material in the cyclic shape memory analysis.

In order to determine at which temperature the SEBS60 as the representative blend performs how much shape recovery, a stepwise shape memory analysis was performed by waiting for 15 min at every 5 °C increase between 40 and 65 °C. The thermomechanical graph of the analysis performed is given in Fig. 5(b) and the shape recovery ratios obtained are given in Table S5 (Supplementary Material File). It is clear from the figure that the SEBS60 blend started its first shape recovery at 50 °C, where it recovered 0.98%. At 55 °C, the shape recovery reached 62.02% as most of the PCL crystals melted. At this temperature, the shape recovery could not be completed because not all crystals melted. When the T_{trans} was 60 °C, one more step occurred and 77.39% recovery was achieved. At 65 °C, although there was no formation of a new shape recovery step, indicating that 60 °C is appropriate as the shape transition temperature, the shape recovery improved further, reaching a value of 79.43%.

Another thermo-responsive shape memory analysis was conducted for the SEBS 60 blend using a sample deformed in a "U" shape. For the analysis, a sample with dimensions of $5.0 \times 0.5 \times 0.1$ cm^3 [Fig. 6(a)] was immersed in hot water at 65 °C for 30 s and then taken out. The heated sample was deformed into a "U" shape with arms spaced 1 cm apart using a 3D printed mold. While the applied load was maintained, the sample was submerged in cold water at 10 °C to preserve the temporary shape. It was observed that the cooled SEBS 60 blend maintained its temporary "U" shape [Fig. 6(b)]. Subsequently, the sample in its temporary shape was placed inside an oven at 65 °C, and the recovery process from the temporary shape to the permanent shape was monitored. The images of the shape recovery process are shown in Fig. 6(c). The SEBS60 blend completely recovered its permanent shape from temporary "U" shape within 330 s. In this analysis, a higher shape recovery was achieved compared to

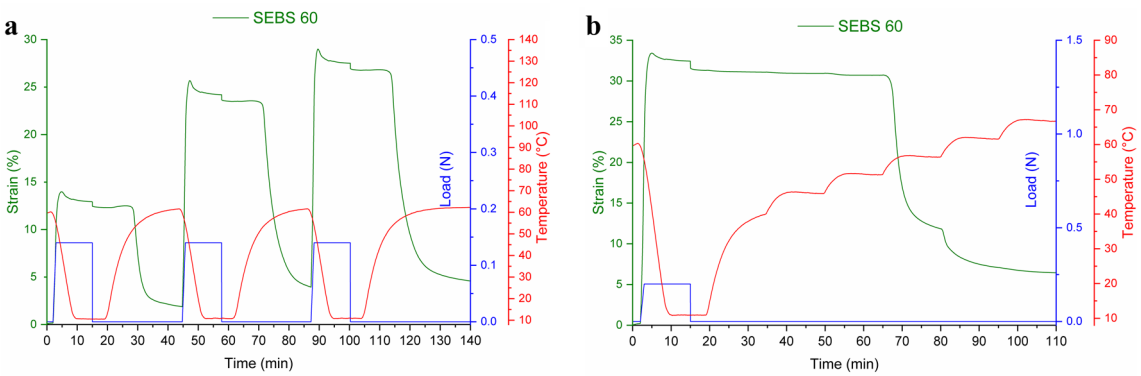

Figure 5: Shape memory performances of SEBS 60 blend under various conditions (a) cyclic shape memory behavior and (b) stepwise shape memory analysis.

© The Author(s), under exclusive licence to The Materials Research Society 2023

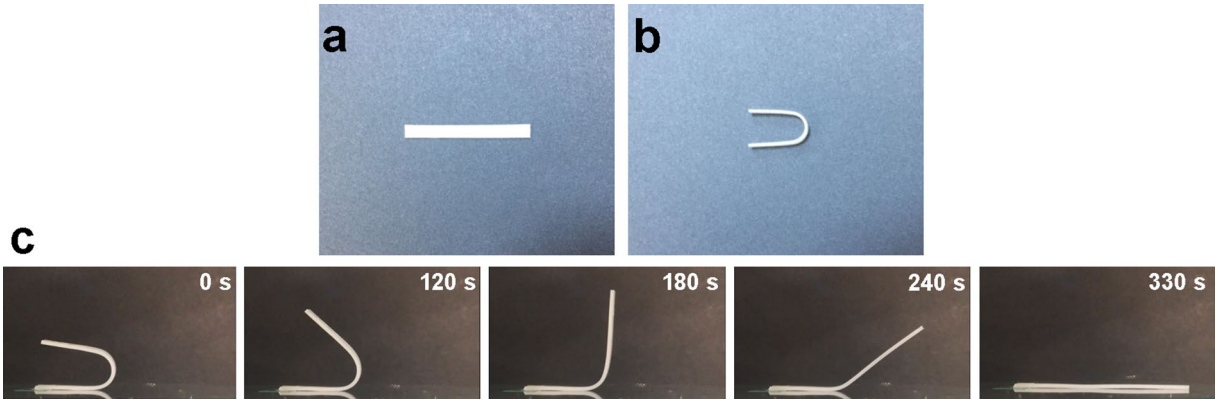

Figure 6: Shape recovery performance of "U-shaped" SEBS 60 blend (a) Permanent shape, (b) Temporary shape, and (c) Shape recovery at 65 °C.

the shape recovery rate obtained from the TMA device (Table 3). This difference can be attributed to the variation in deformation between the two analyses. During the TMA test, the sample underwent long-term deformation in the tensile shape, while for the "U" shape, the sample was subjected to short-term bending deformation. The higher permanent deformation obtained during the tensile deformation might be due to the untangling of the SEBS-g-MA molecules and the loss of their positions over each other as a result of the deformation process, leading to higher permanent deformation. Consequently, the return of elastomer molecules to their original high-entropy states in the TMA device might have been more challenging, resulting in a decreased shape recovery ratio. Recovery process of SEBS60 blend is given as Video S1 (Supplementary Material File) as supplementary material.

Self-healing behavior

The self-healing ability of the SEBS60 polymer blend, as the representative sample, was analyzed, and related photographs and optical microscope images are presented in Fig. 7. In the analysis, the sample with dimensions of $10.0 \times 1.0 \times 0.1$ cm^3 was first damaged by creating a 0.8 cm deep notch using a utility knife [Fig. 7(a)]. Subsequently, the damaged sample with the surfaces of the notch touching each other was placed in an oven at a temperature of 70 °C, a temperature above the melting temperature of the PCL phase and below the glass transition temperature of the PS blocks of the SEBS-g-MA, and allowed to self-healing for 5 min. The sample was then cooled to room temperature [Fig. 7(b)]. The self-healing sample was observed to bend around the notched area, and the damaged area surfaces remained connected without separating from each other, forming a cohesive structure. The sample demonstrated its ability to repair itself successfully [Fig. 7(c)]. In the optical microscope images, it is observed that the notched surfaces, which were separated in the damaged area [Fig. 7(d)], merged after the self-healing process [Fig. 7(e)]. However, the damaged area did not completely disappear. This is due to the fact that the self-healing process was carried out at a temperature well below the flow temperature of the SEBS-g-MA polymer. As a result, only the PCL phase in the blend melted and actively participated in the self-healing process, while the SEBS-g-MA phase did not reach its flow temperature and did not contribute significantly to the healing.

To determine the self-healing property of the SEBS60 polymer blend, tensile tests were conducted at room temperature with a speed of 500 mm/min using notched and self-healed samples. The stress–strain curves for the analysis are presented in Fig. S6 (Supplementary Material File), and the analysis results are given in Table S6 (Supplementary Material File). In the stress–strain curves, it was determined that the elongation at break of the notched sample, which was 8.70%, increased to 74.94% after the self-healing process. Furthermore, the tensile strength improved from 3.18 to 5.17 MPa. The toughness value, which is a measure of the energy required for the material to fail, increased from 73.17 to 1376.66 Nmm. Based on the improvements achieved in the mechanical properties, it can be concluded that the PCL phase acted as an active healing agent for the polymer blend by melting at 70 °C. The results indicate that the SEBS60 polymer blend demonstrates self-healing behavior, where the PCL phase at 70 °C acts as an active repair agent, leading to significant improvements in mechanical properties after the self-healing process.

Conclusion

Static and dynamic mechanical properties as well as thermo-responsive shape memory capabilities of polymer blends having various ratios of SEBS-g-MA and PCL were investigated within the context of this study. The solution blending approach was utilized to create the SEBS-g-MA/PCL blends, with the expectation that favorable interphase interactions would occur between the polar groups present in both polymers. The blends with component ratios of 50/50 and 60/40 (SEBS-g-MA/PCL) displayed co-continuous morphologies, while others exhibited a

© The Author(s), under exclusive licence to The Materials Research Society 2023

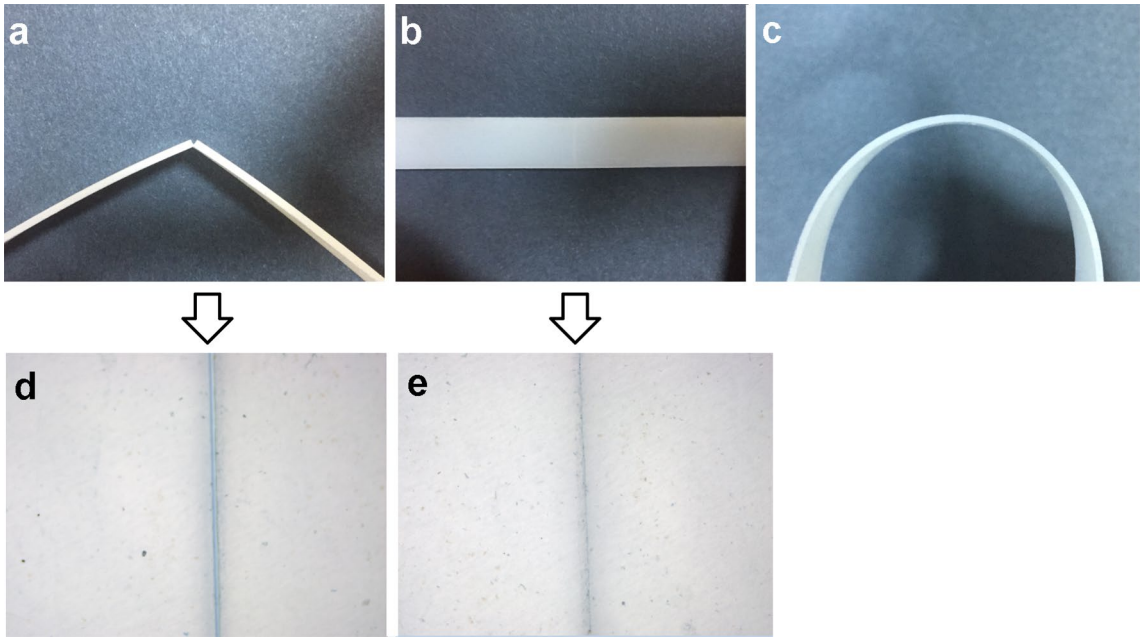

Figure 7: Self-healing application of the SEBS60 blend: (a) Damaged (notched) state, (b) Self-healed state, (c) Bent condition of the healed specimen, (d) Microscope image of damaged (notched) specimen, and (e) Microscope image of self-healed specimen.

discontinuous distribution of the PCL phase in the SEBS-g-MA matrix. The SEBS50 blend, with higher PCL content, achieved the maximum tensile modulus. All blends demonstrated higher elongation compared to SEBS-g-MA but lower elongation than pure PCL. The addition of the hard PCL component reduced the creep deformation in the blends due to the restricted molecular motions of SEBS molecules by PCL domains. Notably, the SEBS50 and SEBS60 blends with co-continuous morphologies and higher PCL concentrations exhibited the lowest damping values at their glass transition temperatures, attributed to limited mobilities of the SEBS chains within the abundant hard PCL phases. Thermo-responsive shape memory analyses revealed that the SEBS60 blend displayed optimum shape fixing and shape recovery values of 97.15 and 76.29%, respectively. This blend demonstrated the ability to maintain its temporary shape and entirely recover to its permanent shape. Additionally, the SEBS60 blend exhibited shape memory repeatability for at least three cycles and showcased self-healing behavior. Self-healing characterization on a sample of SEBS60 revealed a remarkable increase (1780%) in toughness compared to a notched sample. Based on its superior thermoresponsive shape memory properties, the SEBS60 blend was identified as the best composition. Moreover, SEBS-g-MA/PCL shape memory polymer blends hold potential for applications such as self-healing materials and actuators. These findings highlight the potential of SEBS-g-MA/PCL blends as heat-responsive shape memory materials with a diverse range of applications, including smart textiles and biomedical devices. The tunable morphological and mechanical properties of these blends position them as promising candidates for various practical applications requiring shape-memory behavior. Further exploration and optimization of these blends offer exciting prospects for innovative solutions in material design and engineering.

Experimental

Materials

The SEBS-g-MA thermoplastic elastomer with a commercial code FG 1901, containing 30% polystyrene and 1.4–2% maleic anhydride, and having a Shore A hardness of 71, was obtained from Kraton (Texas, USA). The PCL polymer (PCL-6500) with a molecular weight of 50,000 g/mol was provided by Juren Chemical (Yueyang, China). Tetrahydrofuran (THF) was supplied by Merck (Darmstadt, Germany).

Preparation of shape memory SEBS-g-MA/PCL blends by solution mixing

Blends of SEBS-g-MA/PCL polymers with various compositions were prepared using the solution mixing method, with the assistance of THF as a solvent. The polymers were mixed with THF at a weight-to-volume ratio of 1/5 and stirred with a magnetic stirrer for three hours until they were thoroughly dissolved. The resulting polymer solutions were then poured into Teflon molds measuring 10×10 cm^2 and dried for 24 h at room temperature in a fume hood. This process resulted in the formation of films for each composition, with approximately 1 and 0.3 mm thicknesses. The film samples with a thickness of

© The Author(s), under exclusive licence to The Materials Research Society 2023

0.3 mm were used for creep and shape memory tests, while the ones with a thickness of 1 mm were utilized for tensile testing, self-healing, and SEM (Scanning Electron Microscope) analyses. Table S7 (Supplementary Material File) provides information on the compositions and codes of the polymer blends.

Characterization

Scanning electron microscopy (SEM) was used to examine the morphological characteristics of the polymer blends. The samples were broken under liquid nitrogen to preserve their structure and then immersed in dioxane solvent to etch the PCL phase and reveal the phase distribution of the PCL polymer in the blends. The etching process was carried out for 15 min at room temperature. After etching, the SEBS-g-MA/PCL blends were dried for 24 h at 35 °C in a vacuum oven. After the drying process, the samples were further prepared for SEM analysis by coating them with a thin layer of platinum. The coated samples' surfaces were monitored a scanning electron microscope (SEM) (ESEM-FEG/EDAX Philips XL-30 microscope, Philips, Eindhoven, The Netherlands).

The DSC-Q200 (TA Instruments, USA) differential scanning calorimeter (DSC) instrument was employed to determine the transition temperatures and the degree of crystallization in the blends. The heating and cooling rates used during the analysis were set to 10 °C/min, and the measurements were carried out under a nitrogen atmosphere. The analyses consisted of three steps, and endothermic transitions were identified during the second heating cycle. To calculate the crystallization percentage of PCL in the blends, Eq. 1 was utilized.

$$X_c = \frac{\Delta H_f}{\Delta H_{f0}} \times \frac{1}{W} \times 100 \quad (1)$$

In the equation, X_c represents the crystallization percentage, ΔH_f represents the melting enthalpy determined by the analysis, and H_{f0} represents the melting enthalpy of a polymer that is entirely crystalline. W as the weight fraction stands for the amount of the crystalline polymer in the mixture by weight. The PCL's ΔH_{f0} value was used as 139.5 J/g [9]. The DSC thermograms are given in Supplementary Material File (Fig. S1).

Fourier-transform infrared (FTIR) analyses were done out with a Perkin Elmer 1600 FTIR-ATR spectrophotometer (Massachusetts, USA). The FTIR spectra together with their discussion are presented in the Supplementary Material File (Figs. S2 and S3).

The tensile properties of both neat polymers and the polymer blends were tested at room temperature using a 1 kN capacity Zwick/Roell (Zwick, Germany) universal test machine. The tests were conducted at a drawing rate of 500 mm/min. Rectangular samples with dimensions of $10 \times 1 \times 0.1$ cm^3 were used for the analyses.

The creep behavior of the polymer blends and neat polymers was investigated using a thermomechanical analysis (TMA) device (TMA7100, Hitachi, Japan) at 25 °C. In the creep tests, rectangular samples with dimensions of $5 \times 2 \times 0.3$ mm^3 were used. The samples were subjected to a 15-min period of 1 MPa stress, after which the stress was removed, and a subsequent 15-min period of strain recovery was conducted. To study the effect of temperature on the creep behavior of a representative blend, the same process was repeated at 35 and 45 °C.

Dynamic mechanical analyses of the SEBS-g-MA/PCL polymer blends were conducted using samples with dimensions of $5.0 \times 2.0 \times 0.3$ mm^3. The tests were performed at a frequency of 0.1 Hz and in tension mode using a thermomechanical analyzer (TMA) (TMA7100, Hitachi, Japan) equipped with an electrical cooling system. The analyses were carried out over a temperature range of − 62 to 70 °C, with a heating rate of 3 °C/min.

Using the thermomechanical analysis (TMA) instrument (TMA7100, Hitachi, Japan), the samples with dimensions of $5.0 \times 2.0 \times 0.3$ mm^3 were used for the thermo-responsive shape memory analyses of the polymer blends. Tensile mode and the force control process were used during the test. Four stages were conducted to apply the test method; (a) *The first stage (deformation):* The test sample was heated to 60 °C, which is the shape transition temperature (T_{trans}) identified by DSC analysis, just above the T_m of PCL, and left there for 1 min until the temperature achieved equilibrium. The sample was then subjected to a strain (ε_m) value which is between 40 and 50% by exerting force at a stationary speed, (b) *The second stage (shape fixing):* By keeping the applied force on the deformed sample, it was cooled to 10 °C, which is the shape-fixing temperature (T_{fix}), where PCL crystallization was complete. After waiting at this temperature for five minutes, the temporary shape was gained, (c) *The third stage (removal of force):* The fixed amount of deformation (ε_f) at which the material could maintain its temporary shape was calculated in this stage by removing the force applied to the sample at T_{fix} temperature and waiting for 5 min, (d) *Fourth stage (Shape Recovery):* The fixed-shape sample was heated to 60 °C (T_{trans}) at a heating rate of 10 °C, and the material's ability to regain its original shape was evaluated after 40 min. Following the shape recovery stage, the material's permanent deformation (strain) (ε_r) was calculated. Afterward, using Eqs. 2 and 3, the values of the blends' shape recovery ratio (R_r) and shape fixing ratio (R_f) were determined [31].

$$R_r = \frac{\varepsilon_m - \varepsilon_r}{\varepsilon_m} \times 100 \quad (2)$$

$$R_f = \frac{\varepsilon_f}{\varepsilon_m} \times 100 \quad (3)$$

© The Author(s), under exclusive licence to The Materials Research Society 2023

Also, the chosen polymer blend underwent three cycles of the thermo-responsive shape memory test, and during each of those repeats, changes in the polymer's capacity to retain shape were assessed. The shape recovery ratios were calculated by waiting 15 min for each temperature with a 5 °C difference between 40 and 65 °C to find how much shape recovery the polymer blend provides at which temperature.

The self-healing capacity of the chosen blend was ascertained using a utility knife to cut a notch of $10.0 \times 1.0 \times 0.1 cm^3$ on the sample. The notched sample was placed in an oven set to 70 °C for 5 min while in contact with the notch surfaces, after which it was removed and allowed to cool to room temperature. Using notched and self-healing specimens, tensile tests were carried out at room temperature with a drawing rate of 500 mm/min.

Acknowledgments

Supports given by The Scientific and Technological Research Council of Türkiye (TUBITAK) (Project No. 221M074) and Yalova University Scientific Research Projects Coordination Department are gratefully acknowledged.

Author contributions

ET: conceptualization, supervision, methodology design, writing-reviewing-editing of the manuscript, material preparation, and characterizations of the materials. SŞ: writing-reviewing-editing of the manuscript, and characterizations of the materials.

Funding

This work was supported by The Scientific and Technological Research Council of Türkiye (TUBITAK) (Project No. 221M074) and Yalova University Scientific Research Projects Coordination Department.

Data availability

The data are not publicly available.

Code availability

Not applicable.

Declarations

Conflicts of interest The authors declare that they have no known competing financial interests or personal relationships that could have appeared to influence the work reported in this paper.

Ethical approval

Not applicable.

Supplementary Information

The online version contains supplementary material available at https://doi.org/10.1557/s43578-023-01225-0.

References

1. H. Meng, G. Li, A review of stimuli-responsive shape memory polymer composites. Polymer **54**(9), 2199 (2013). https://doi.org/10.1016/j.polymer.2013.02.023
2. W. Wang, Y. Liu, J. Leng, Recent developments in shape memory polymer nanocomposites: actuation methods and mechanisms. Coord. Chem. Rev. **320**, 38 (2016). https://doi.org/10.1016/j.ccr.2016.03.007
3. A. Ben Abdallah, F. Gamaoun, A. Kallel, A. Tcharkhtchi, Molecular weight influence on shape memory effect of shape memory polymer blend (poly (caprolactone)/styrene-butadiene-styrene). J. Appl. Polym. Sci. **138**(5), 49761 (2021). https://doi.org/10.1002/app.49761
4. J. Li, T. Liu, S. Xia, Y. Pan, Z. Zheng, X. Ding, Y. Peng, A versatile approach to achieve quintuple-shape memory effect by semi-interpenetrating polymer networks containing broadened glass transition and crystalline segments. J. Mater. Chem. **21**(33), 12213 (2011). https://doi.org/10.1039/C1JM12496J
5. E. Tekay, Thermo-responsive shape memory behavior of poly (styrene-b-isoprene-b-styrene)/ethylene-1-octene copolymer thermoplastic elastomer blends. Polym. Adv. Technol. **32**(1), 428 (2021). https://doi.org/10.1002/pat.5139
6. S. Song, J. Feng, P. Wu, A new strategy to prepare polymer-based shape memory elastomers. Macromol. Rapid Commun. **32**(19), 1569 (2011). https://doi.org/10.1002/marc.201100298
7. E. Tekay, Isıl-duyarlı şekil hafızalı kopoliester termoplastik elastomer (COPE) ve poli (etilen-ko-vinil asetat)(EVA) polimer harmanlarının hazırlanması. Fac. Eng. Archit. Gazi Univ. **36**(1), 241 (2020). https://doi.org/10.17341/gazimmfd.722364
8. S.A. Abdullah, A. Jumahat, N.R. Abdullah, L. Frormann, Determination of shape fixity and shape recovery rate of carbon nanotube-filled shape memory polymer nanocomposites. Procedia Eng. **41**, 1641 (2012). https://doi.org/10.1016/j.proeng.2012.07.362
9. X. Jing, H.-Y. Mi, H.-X. Huang, L.-S. Turng, Shape memory thermoplastic polyurethane (TPU)/poly (ε-caprolactone)(PCL) blends as self-knotting sutures. J. Mech. Behav. Biomed. Mater. **64**, 94 (2016). https://doi.org/10.1016/j.jmbbm.2016.07.023
10. C. Schmidt, K. Neuking, G. Eggeler, Functional fatigue of shape memory polymers. Adv. Eng. Mater. **10**(10), 922 (2008). https://doi.org/10.1002/adem.200800213
11. Y. Guo, J. Ma, Z. Lv, N. Zhao, L. Wang, Q. Li, The effect of plasticizer on the shape memory properties of poly (lactide acid)/poly (ethylene glycol) blends. J. Mater. Res. **33**(23), 4101 (2018). https://doi.org/10.1557/jmr.2018.359

© The Author(s), under exclusive licence to The Materials Research Society 2023

12. K.P. Mineart, S.S. Tallury, T. Li, B. Lee, R.J. Spontak, Phase-change thermoplastic elastomer blends for tunable shape memory by physical design. Ind. Eng. Chem. Res. **55**(49), 12590 (2016). https://doi.org/10.1021/acs.iecr.6b04039
13. G. Holden, E. Bishop, N.R. Legge, Thermoplastic elastomers. J. Polym Sci Part C **26**, 37 (1969)
14. A. Wilkinson, M. Clemens, V. Harding, The effects of SEBS-g-maleic anhydride reaction on the morphology and properties of polypropylene/PA6/SEBS ternary blends. Polymer **45**(15), 5239 (2004). https://doi.org/10.1016/j.polymer.2004.05.033
15. Z. Kordjazi, N.G. Ebrahimi, Rheological behavior of noncompatibilized and compatibilized PP/PET blends with SEBS-g-MA. J. Appl. Polym. Sci. **116**(1), 441 (2010). https://doi.org/10.1002/app.31471
16. W. Liu, R. Zhang, M. Huang, X. Dong, W. Xu, N. Ray, J. Zhu, Design and structural study of a triple-shape memory PCL/PVC blend. Polymer **104**, 115 (2016). https://doi.org/10.1016/j.polymer.2016.09.079
17. E.G. Choubar, M.H. Nasirtabrizi, F. Salimi, N. Sohrabi-gilani, A. Sadeghianamryan, Fabrication and in vitro characterization of novel co-electrospun polycaprolactone/collagen/polyvinylpyrrolidone nanofibrous scaffolds for bone tissue engineering applications. J. Mater. Res. **37**(23), 4140 (2022). https://doi.org/10.1557/s43578-022-00778-w
18. A. Sali, S. Duzyer Gebizli, G. Goktalay, Silymarin-loaded electrospun polycaprolactone nanofibers as wound dressing. J. Mater. Res. **38**(8), 2251 (2023). https://doi.org/10.1557/s43578-023-00959-1
19. W. Kuang, P.T. Mather, A latent crosslinkable PCL-based polyurethane: synthesis, shape memory, and enzymatic degradation. J. Mater. Res. **33**(17), 2463 (2018). https://doi.org/10.1557/jmr.2018.220
20. H. Zhang, H. Wang, W. Zhong, Q. Du, A novel type of shape memory polymer blend and the shape memory mechanism. Polymer **50**(6), 1596 (2009). https://doi.org/10.1016/j.polymer.2009.01.011
21. E. Tekay, Preparation and characterization of electro-active shape memory PCL/SEBS-g-MA/MWCNT nanocomposites. Polymer **209**, 122989 (2020). https://doi.org/10.1016/j.polymer.2020.122989
22. B. Peng, Y. Yang, T. Ju, K.A. Cavicchi, Fused filament fabrication 4D printing of a highly extensible, self-healing, shape memory elastomer based on thermoplastic polymer blends. ACS Appl. Mater. Interfaces **13**(11), 12777 (2020). https://doi.org/10.1021/acsami.0c18618
23. E. Tekay, S. Şen, M.A. Korkmaz, N. Nugay, Preparation and characterization of thermo-responsive shape memory ester-based polymer blends. J. Mater. Sci. **58**(19), 8241 (2023). https://doi.org/10.1007/s10853-023-08549-6
24. R. Nehra, S.N. Maiti, J. Jacob, Analytical interpretations of static and dynamic mechanical properties of thermoplastic elastomer toughened PLA blends. J. Appl. Polym. Sci. **135**(1), 45644 (2018). https://doi.org/10.1002/app.45644
25. M. Vanneste, G. Groeninckx, Ternary blends of PCL, SAN15 and SMA14: miscibility, crystallization and melting behaviour, and semicrystalline morphology. Polymer **36**(22), 4253 (1995). https://doi.org/10.1016/0032-3861(95)92221-Y
26. S. Moradi, J.K. Yeganeh, Highly toughened poly (lactic acid) (PLA) prepared through melt blending with ethylene-co-vinyl acetate (EVA) copolymer and simultaneous addition of hydrophilic silica nanoparticles and block copolymer compatibilizer. Polym. Test. **91**, 106735 (2020). https://doi.org/10.1016/j.polymertesting.2020.106735
27. M. Kashif, Y.-W. Chang, Triple-shape memory effects of modified semicrystalline ethylene–propylene–diene rubber/poly (ε-caprolactone) blends. Eur. Polym. J. **70**, 306 (2015). https://doi.org/10.1016/j.eurpolymj.2015.07.026
28. M. Sabzi, M. Babaahmadi, M. Rahnama, Thermally and electrically triggered triple-shape memory behavior of poly (vinyl acetate)/poly (lactic acid) due to graphene-induced phase separation. ACS Appl. Mater. Interfaces **9**(28), 24061 (2017). https://doi.org/10.1021/acsami.7b02259
29. D. Ponnamma, K.K. Sadasivuni, M. Strankowski, P. Moldenaers, S. Thomas, Y. Grohens, Interrelated shape memory and Payne effect in polyurethane/graphene oxide nanocomposites. RSC Adv. **3**(36), 16068 (2013). https://doi.org/10.1039/C3RA41395K
30. S.M. Lai, X.F. Wang, Shape memory properties of olefin block copolymer (OBC)/poly (ε-caprolactone)(PCL) blends. J. Appl. Polym. Sci. **134**(44), 45475 (2017). https://doi.org/10.1002/app.45475
31. Y. Wei, R. Huang, P. Dong, X.-D. Qi, Q. Fu, Preparation of polylactide/poly (ether) urethane blends with excellent electro-actuated shape memory via incorporating carbon black and carbon nanotubes hybrids fillers. Chin. J. Polym. Sci. **36**, 1175 (2018). https://doi.org/10.1007/s10118-018-2138-3

Publisher's Note Springer Nature remains neutral with regard to jurisdictional claims in published maps and institutional affiliations.

Springer Nature or its licensor (e.g. a society or other partner) holds exclusive rights to this article under a publishing agreement with the author(s) or other rightsholder(s); author self-archiving of the accepted manuscript version of this article is solely governed by the terms of such publishing agreement and applicable law.

© The Author(s), under exclusive licence to The Materials Research Society 2023